On reconfiguring radial trees

Yoshiyuki Kusakari

Akita Prefectural University, Honjo Akita, 015-0055, Japan
Kusakari@akita-pu.ac.jp

Abstract. A linkage is a collection of line segments, called bars, possibly joined at their ends, called joints. Straightening a tree linkage is a continuous motion of their bars from an initial configuration to a "straight line segment," preserving the length of each bar and excepting crossing any two bars. In this paper, we introduce a new class of linkages, called "radial trees," and show that there exists a radial tree which can not be straightened.

1 Introduction

A *linkage* is a collection of line segments, called *bars*, possibly joined at their ends, called *joints*. A linkage is called *planar* if all bars are in the plane $\mathbb{R}^2$ with no self-intersection. A *reconfiguration* of a linkage is a continuous motion of their bars, or equivalently a continuous motion of their joints, that preserves the length of each bar. A reconfiguration of a linkage is called *planar* if all bars are in the plane during the motion, and is called *non-crossing* if any two bars do not cross each other during the motion. In this paper, we consider only a planar reconfiguration of a planar linkage, and we may omit the word "planar." Furthermore, we consider only a non-crossing reconfiguration, and we may omit the word "non-crossing."

For such planar reconfiguration problems, there is a fundamental question: whether any polygonal chain can be *straightened*. This problem had been open from the 1970's to the 1990's. However, Connelly et al. have answered this question affirmatively: they show that any polygonal chain can be straightened [3]. On the other hand, a negative result is known for a non-crossing planar reconfiguration of a tree linkage: there exists a tree which cannot be "straightened" [1, 2]. Figure 1 illustrates a tree which cannot be straightened [1, 2]. Recently, an affirmative result is reported for reconfiguring tree linkages: Kusakari et al. show that any "monotone tree" can be straightened, and give a method for straightening "monotone trees"[4]. Figure 2 illustrates a monotone tree [4]. It is desired to characterize the class of trees which can be straightened.

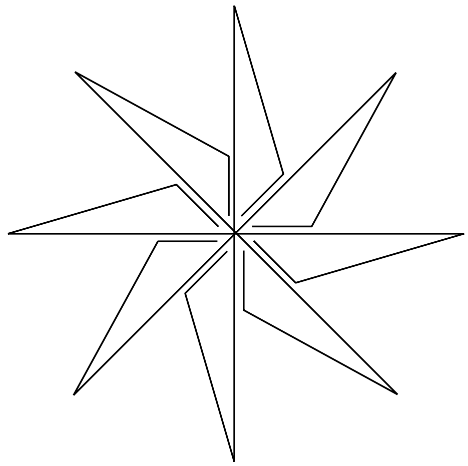

Figure 1. Locked tree.

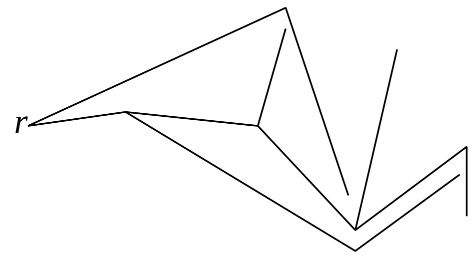

Figure 2. Monotone tree.

In this paper, we define a new class of trees, called “radially monotone trees” or “radial trees,” which is a natural modification of the class of monotone trees, and show that there exists a radial tree which cannot be straightened. The remainder of this paper is organized as follows. In Section 2, we give some preliminary definitions. In Section 3, we give a method to construct a locked radial tree. In Section 4, we show that the initial tree constructed in Section 3 is simple and radial. In Section 5, we show that the tree constructed in Section 3 can not be straightened. Finally, we conclude in Section 6.

2 Preliminaries

In this section, we define terms and formally describe our problem.

Let $L = (J, B)$ be a linkage consisting of a joint set J and a bar set B. A structural graph of a linkage L is denoted by $SG(L)$. An embedding of a structural graph $SG(L)$ is called a *configuration* of linkage L. A linkage L is called a *(rooted) tree linkage* or a *(rooted) tree* if the structural graph $SG(L)$ is a (rooted) tree. Let $T = (J, B)$ be such a rooted tree linkage, and $r \in J$ be the root of T. A bar $b \in B$ is denoted by (j_s, j_t) if $j_s \in J$ is the parent of $j_t \in J$. For any joint $j \in J$, an incident bar $b = (j, j')$ is called a *child bar of joint* j. A *leaf* is a joint having no child bar. For any joint $j \in J - \{r\}$, an incident bar $b = (j', j)$ is called a *parent bar of joint* j. For any joint $j \in J - \{r\}$, a parent bar of j is unique, and is denoted by $\bar{j}$. A joint $j \in J$ is *internal* if j is neither the root nor a leaf. A *straightened configuration of a rooted tree linkage* is one in which, for any internal joint j, the parent bar $\bar{j}$ of j makes angle π with each child bar of j, and the angle between each pair of child bars of j is zero. *Straightening a tree linkage* T is a reconfiguration of T from an initial configuration to a straightened configuration.

For an initial configuration of a tree linkage, we first describe a definition of a monotone tree [4]. A polygonal chain P is *x-monotone* if the intersection of P and any vertical line is either a single point or a line segment if the intersection is not empty. A configured tree T is *x-monotone* if T is a rooted tree and the polygonal chain in T from the root r to any leaf is x-monotone. (See Figure 2.) Next, we define radial trees by slightly modifying the definition of monotone trees. A polygonal chain P is *radially monotone (for a point p)* or *radial (for a point p)* if the intersection of P and any circle with the same center p is either a single point or empty. A tree T is *radially monotone* or *radial* if T is a rooted tree and the directed polygonal chain in T from the root r to any leaf is radially monotone for the root r. A radial tree is illustrated in Figure 3. Note that an x-monotone tree may not be radial, and a radial tree may not be x-monotone.

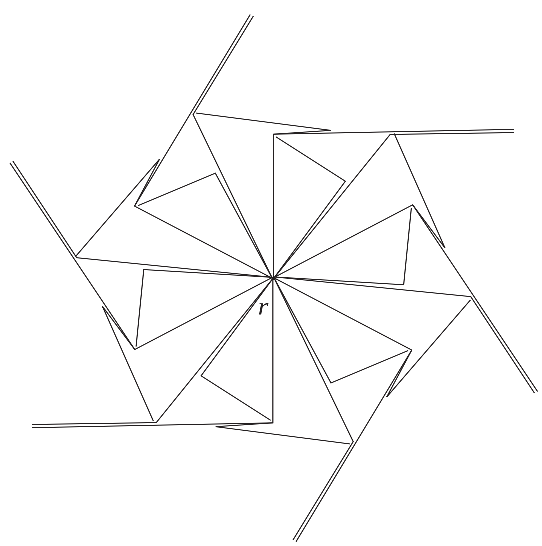

Figure 3. Locked radial tree.

For three points $p_1, p_2, p_3 \in \mathbb{R}^2$, the angle $\angle p_1p_2p_3$ is measured counterclockwise from the direction of $\overrightarrow{p_2p_1}$ to the direction of $\overrightarrow{p_2p_3}$, and ranges in $[0, 2\pi)$. For two bars $\bar{j_1} = (j_0, j_1), \bar{j_2} = (j_1, j_2) \in B$ joined with joint j_1, the angle $\angle j_0j_1j_2$ is denoted by $\theta(\bar{j_1}\bar{j_2})$. The *slope* $s(\bar{j_1})$ of bar $\bar{j_1} = (j_0, j_1)$ is the angle measured counterclockwise at the parent joint j_0 from $+x$ direction to the direction $\overrightarrow{j_0j_1}$, and ranges in $[0, 2\pi)$. Thus,the following equation holds:

$$\theta(\bar{j_1}\bar{j_2}) = s(\bar{j_2}) - s(\bar{j_1}) + 2\pi \pmod{2\pi}.$$

The length of bar b is denoted by $|b|$. For two points $p_1, p_2 \in \mathbb{R}^2$, the ray starting from p_1 and passing through p_2 is denoted by $R(p_1, p_2)$. For a point $p \in \mathbb{R}^2$ and a direction $d \in [0, 2\pi)$, the ray starting from p and going in the direction d is denoted by $R_p(d)$.

3 Constructing a Locked Radial Tree

In this section, we construct a radial tree which can not be straightened, i.e., we construct a *locked* radial tree. Figure 3 illustrates such a locked radial tree.

3.1 Overview

The locked tree T in Figure 3 contains six congruent components C_0, C_1, $\cdots$, C_5, all of which are joined at the root r of T. More generally, one can construct a locked radial tree by such $n(> 4)$ congruent components, each of which is called a C_i*-component* and is often denoted by C_i, for i,$0 \le i \le n-1$. Each C_i-component consists of three subcomponents: a V_i*-component*, an L_i*-component* and a Γ_i*-component*. These V_i-component, L_i-component and Γ_i-component are often denoted by V_i,L_i and Γ_i, respectively. For each i,$0 \le i \le n-1$, these V_i,L_i and Γ_i are incident to the root r counterclockwise in this order. Furthermore, L_i is wrapped by V_i and Γ_i, as illustrated in Figure 4.

A V_i-component has two bars $\bar{v_1} = (v_0, v_1), \bar{v_2} = (v_1, v_2)$ joined with the internal joint v_1 whose angle $\theta(\bar{v_1}\bar{v_2})$ is nearly $\frac{\pi}{2} + \frac{\pi}{n}(= \frac{\pi}{2} + \frac{\pi}{6})$, and looks like the letter "V", as illustrated in Figure 5. An L_i-component has two bars $\bar{l_1} = (l_0, l_1), \bar{l_2} = (l_1, l_2)$ joined with the internal joint l_1 whose angle $\theta(\bar{l_1}\bar{l_2})$ is nearly $\frac{3\pi}{2}$, and looks like the letter "L", as illustrated in Figure 6. A Γ_i-component has four bars $\bar{\gamma_1} = (\gamma_0, \gamma_1)$, $\bar{\gamma_2} = (\gamma_1, \gamma_2)$, $\bar{\gamma_3} = (\gamma_1, \gamma_3)$ and $\bar{\gamma_4} = (\gamma_3, \gamma_4)$, and two internal joints γ_1, γ_3, and looks like the letter "Γ", as illustrated in Figure 7. The angles $\angle\gamma_0\gamma_1\gamma_2$, $\angle\gamma_0\gamma_1\gamma_3$ and $\angle\gamma_0\gamma_3\gamma_4$ are nearly $\frac{\pi}{2}$,$\frac{\pi}{2}$ and $\frac{3\pi}{2}$, respectively.

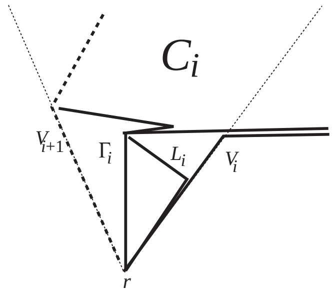

Figure 4. Component C_i.

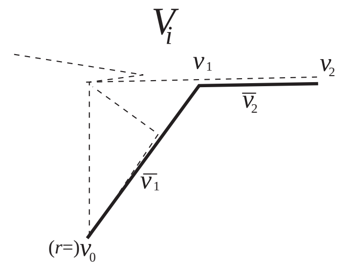

Figure 5. Subcomponent V_i.

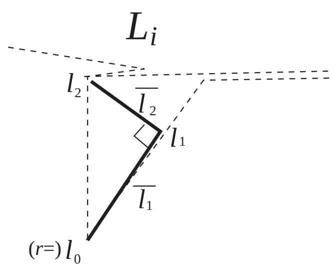

Figure 6. Subcomponent L_i.

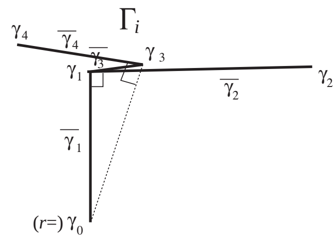

Figure 7. Subcomponent Γ_i.

3.2 A detail of the construction

In this subsection, we focus on a single C_i-component, and may often omit the index i for simplification. Furthermore, subcomponents, bars, and joints in C_{i-1} or C_{i+1} are designated by the corresponding notation with symbol "-" or "+", respectively. For example, Γ_{i-1}, Γ_i and Γ_{i+1} are denoted by Γ^-, Γ and Γ^+, respectively. Moreover, the bar in Γ_{i+1} corresponding to the bar $\bar{\gamma_1}$ in Γ_i is denoted by $\bar{\gamma_1}^+$. We use similar notations for the others. For two points $p_1, p_2 \in \mathbb{R}^2$, we use p_1p_2 to designate the line segment between p_1 and p_2, and $|p_1p_2|$ to denote the length of the segment p_1p_2.

We will draw a figure C_i^* containing the initial configuration of the C_i-component. In order to designate each points or segments in C_i^*, we use the notation adding symbol "*" to the corresponding notation of the joint $j \in J$ or the bar $b \in B$. Note that, for i, $0 \leq i \leq n-1$, we draw all figures C_i^* simultaneously, so that each pair of corresponding bars in consequent components makes angle $\frac{2\pi}{n}$, and the index i increases counterclockwise. Without loss of generality, we may assume that the length $|\bar{\gamma_1}^*| = 1$, and the slope $s(\bar{\gamma_1}^*) = \frac{\pi}{2}$. Renote that we first draw all bars corresponding to $\bar{\gamma_1}^*$ for all C_i^* simultaneously. Then, we draw a line segment $\bar{\gamma_2}^*$ from the point γ_1^* with the slope $s(\bar{\gamma_2}^*)$, so that the angle $\theta(\bar{\gamma_1}^*\bar{\gamma_2}^*) = \frac{\pi}{2}$. We choose the length $|\bar{\gamma_2}^*|$ long enough, so that the ray $R(r, {\gamma_1^-}^*)$ intersects $\bar{\gamma_2}^*$. Thus, we choose $|\bar{\gamma_2}^*| > \tan(\frac{2\pi}{n})$. Next, we choose a point γ_4^* on the bar $\bar{\gamma_2}^{+*}$, so that the following equation holds:

$$\tan(\frac{\pi}{n}) < |\gamma_1^{+*}\gamma_4^*| < \min\{\tan(\frac{2\pi}{n}), \frac{1}{\sin(\frac{2\pi}{n})}\}. \qquad (1)$$

Then, we can find the point γ_3^* on the bar $\bar{\gamma_2}^*$ satisfying $\angle r\gamma_3^*\gamma_4^* = \frac{3\pi}{2}$. We draw two line segments $\gamma_4^* r$ and $\gamma_4^*\gamma_3^*$. We finally drop a perpendicular from γ_1^* to $r{\gamma_4^-}^*$ and the foot of the perpendicular is l_1^*.

We construct C_i on the figure C_i^*. The notation $j \approx p$ denote that joint j is configured sufficiently near point p, and the notation $b \approx s$ also denote that bar b is configured sufficiently near line segment s. The initial configuration of the C_i-component is obtained as follows:for the V_i-components, let $\bar{v_1} \approx \bar{v_1}^* = r{\gamma_4^-}^*$ and $\bar{v_2} \approx \bar{v_2}^* = {\gamma_4^-}^*\gamma_2^*$; for the L_i-components, let $\bar{l_1} \approx \bar{l_1}^* = rl_1^*$ and $\bar{l_2} \approx \bar{l_2}^* = l_1^*\gamma_1^*$; for the Γ_i-components, $\bar{\gamma_1} \approx \bar{\gamma_1}^* = r\gamma_1^*$, $\bar{\gamma_2} \approx \bar{\gamma_2}^* = \gamma_1^*\gamma_2^*$, $\bar{\gamma_3} \approx \bar{\gamma_3}^* = \gamma_1^*\gamma_3^*$ and $\bar{\gamma_4} \approx \bar{\gamma_4}^* = \gamma_3^*\gamma_4^*$. (See Figure 4.)

4 The initial configuration

In this section, we show that the tree constructed in the previous section is simple and radial. From now on, we often do not distinguish between the linkage and its configuration, and may often omit the symbol "*."

4.1 Simplicity

The slope $s(\bar{\gamma_2}^+) = \frac{2\pi}{n} < \frac{\pi}{2}$ if $n > 4$, and hence the ray $R_{\gamma_1}(\frac{\pi}{2})$ must cross $\bar{\gamma_2}^+$. Let X be the intersection point of the ray $R_{\gamma_1}(\frac{\pi}{2})$ with $\bar{\gamma_2}^+$, and let Y the intersection point of the ray $R_{\gamma_1}(\pi)$ with $\bar{\gamma_2}^+$, as illustrated in Figure 8. Since $|\bar{\gamma_1}^+| = 1$ and $\angle Xr\gamma_1^+ = \angle\gamma_1 r\gamma_1^+ = \frac{2\pi}{n}$, $|\gamma_1^+X| = \tan(\frac{2\pi}{n})$. Furthermore, one can observe that $|\gamma_1^+Y| = \tan(\frac{\pi}{n})$ as follows: since the hypotenuses are common and $|r\gamma_1| = |r\gamma_1^+| = 1$, two right triangles $\triangle rY\gamma_1$ and $\triangle rY\gamma_1^+$ are congruent, and hence $\angle\gamma_1 rY = \angle Yr\gamma_1^+ = \frac{\pi}{n}$. By equation (1), $\tan(\frac{\pi}{n}) < |\gamma_1^{+*}\gamma_4^*| < \tan(\frac{2\pi}{n})$, and hence the point γ_4^* is contained in the open line segment XY. Thus, one can observe that the two line segments $\gamma_4^* r(= \bar{v_1}^{+*})$ and $\gamma_4^*\gamma_3^*(= \bar{\gamma_4}^*)$ can be drawn without crossing any other line segments. Furthermore, one can observe that any pair of line segments in C_i^* can be drawn without crossing even if the pair contains neither $\bar{v_1}^{+*}$ nor $\bar{\gamma_4}^*$. Therefore, the tree constructed in Section 3 is simple.

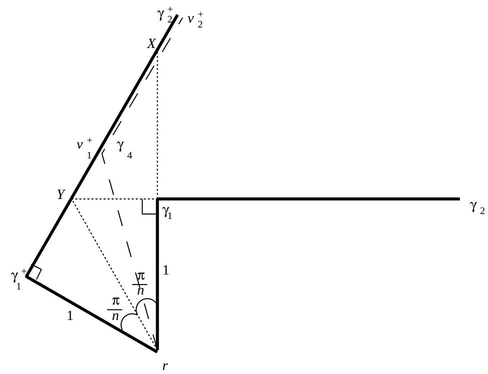

Figure 8. Position of v_1^+.

4.2 Radial Monotonicity

For any joint $j \in J$, a subtree of T rooted at j is denoted by $T(j)$. For any configured joint $j \in \mathbb{R}^2$, the circle with the center o passing through j is denoted by $C_o(j)$. A *wedge* p_1jp_2 is the set of points swept out by a ray starting j moving counterclockwise from the direction $\overrightarrow{jp_1}$ to the direction $\overrightarrow{jp_2}$, and contains points on both $R(j,p_1)$ and $R(j,p_2)$. A wedge p_1jp_2 may be denoted by $w_j[\theta_1,\theta_2]$, where $\theta_1 = \angle rjp_1$, $\theta_2 = \angle rjp_2$, and r is the root of the tree T.

The following lemmas hold.

Lemma 1. (i) *A tree $T = (J,B)$ is radial if and only if, for any joint $j \in J$, all joints j' (except j) in the subtree $T(j)$ are properly outside of $C_r(j)$.*

(ii) *A tree $T = (J,B)$ is radial if and only if, for any joint $j \in J - \{r\}$, a child bar $b = (j,j') \in B$ is contained in the wedge $w_j[\frac{\pi}{2}, \frac{3\pi}{2}]$.*

Proof. Both (i) and (ii) are obvious from the definition of radial trees. □

Note that, for any bar $b = (r,j)$ incident to the root r, the slope $s(b)$ can be taken any values in $[0, 2\pi)$ even if T is radial.

Lemma 2. (i) *A V_i-component is radial for the root r.*

(ii) *An L_i-component is radial for the root r.*
(iii) *A Γ_i-component is radial monotone for the root r.*

Proof. (i) One can easily observe that the angle $\theta(\bar{v_1}\bar{v_2}) \geq \frac{\pi}{2}$. (See Figure 5.) Thus, $\bar{v_2} \subseteq w_{v_1}[\frac{\pi}{2}, \frac{3\pi}{2}]$, and hence the path $(r =)v_0v_1v_2$ is radial by Lemma 1 (ii).
(ii) From the construction of a L_i-component, $\theta(\bar{l_1}\bar{l_2}) = \frac{3\pi}{2}$. Thus, $\bar{l_2} \subseteq w_{l_1}[\frac{\pi}{2}, \frac{3\pi}{2}]$, and hence the path $(r =)l_0l_1l_2$ is radial by Lemma 1 (ii).
(iii) Since a Γ_i-component has two leaves, and hence it is sufficient to show that both path $P_1 = \gamma_0\gamma_1\gamma_2$ and path $P_2 = \gamma_0\gamma_1\gamma_3\gamma_4$ are radial. From the construction, $\theta(\bar{\gamma_1}\bar{\gamma_2}) = \frac{\pi}{2}$, and hence P_1 is radial by Lemma 1 (ii). Furthermore, one can observe that $\bar{\gamma_3} \subseteq w_{\gamma_1}[\frac{\pi}{2}, \frac{3\pi}{2}]$ and $\bar{\gamma_4} \subseteq w_{\gamma_3}[\frac{\pi}{2}, \frac{3\pi}{2}]$ since $\theta(\bar{\gamma_1}\bar{\gamma_3}) = \frac{\pi}{2}$ and $\angle\gamma_0\gamma_3\gamma_4 = \frac{3\pi}{2}$. Thus, by Lemma 1 (ii), P_2 is radial. $\square$

Any C_i-component is radial since all subcomponents are radial by Lemma 2 above, and hence the tree constructed in Section 3 is radial.

5 Lockableness

In this section, we show that the tree constructed in Section 3 can not be straightened.

For the sake of simplicity, we assume that $|\bar{v_1}| = |\bar{v_1}^*|$, $|\bar{v_2}| = |\bar{v_2}^*|$, $|\bar{l_1}| = |\bar{l_1}^*|$, $|\bar{l_2}| = |\bar{l_2}^*|$, $|\bar{\gamma_1}| = |\bar{\gamma_1}^*|$, $|\bar{\gamma_2}| = |\bar{\gamma_2}^*|$, $|\bar{\gamma_3}| = |\bar{\gamma_3}^*|$ and $|\bar{\gamma_4}| = |\bar{\gamma_4}^*|$. Note that each pair of bars does not "properly cross" each other even if lengths of bars are chosen by above way and the initial configuration of C_i is embedded on C_i^*. Furthermore, all lengths $|\bar{\gamma_3}|$, $|\bar{v_1}|$, $|\bar{l_1}|$ and $|\bar{l_2}|$ are determined if $|\gamma_1^+\gamma_4|$ is determined. Thus, there are no choice of lengths for bars $\bar{\gamma_3}$, $\bar{v_1}$, $\bar{l_1}$ and $\bar{l_2}$.

For the initial configuration, the following lemma holds.

Lemma 3. *The following four equations hold:*

(i) $\angle r\gamma_1 l_1 < \frac{\pi}{2}$,
(ii) $\angle l_1\gamma_1\gamma_2 < \frac{\pi}{2}$,
(iii) $\angle r\gamma_4\gamma_3 < \frac{\pi}{2}$, *and*
(iv) $\angle\gamma_3\gamma_4 v_2^+ < \frac{\pi}{2}$.

Proof. Since $\angle r\gamma_1\gamma_2 = \angle r\gamma_1 l_1 + \angle l_1\gamma_1\gamma_2 = \frac{\pi}{2}$, both (i) and (ii) immediately hold. Moreover, since $\angle\gamma_4\gamma_3 r = \frac{\pi}{2}$ and $\angle\gamma_4\gamma_3 r + \angle\gamma_3 r\gamma_4 + \angle r\gamma_4\gamma_3 = \pi$, (iii) holds. Thus,we only prove (iv) below.

For the quadrangle $\square r\gamma_3\gamma_4\gamma_1^+$, $\angle\gamma_4\gamma_3 r = \angle r\gamma_1^+\gamma_4 = \frac{\pi}{2}$ from our construction of the tree, and hence $\angle\gamma_1^+\gamma_4\gamma_3 + \angle\gamma_3 r\gamma_1^+ = \pi$. Let Z and

W be vertices of a rectangle $\Box rZW\gamma_1^+$ such that the vertex Z is on $\bar{\gamma_2}$ and the vertex W is on $\bar{\gamma_2^+}$, as illustrated in Figure 9. Then, $\angle\gamma_1 Zr = \angle\gamma_1 r\gamma_1^+ = \frac{2\pi}{n}$, since $\angle Zr\gamma_1 + \gamma_1 Zr = \angle Zr\gamma_1 + \angle\gamma_1 r\gamma_1^+ = \frac{\pi}{2}$. Therefore, $|\gamma_1^+ W| = |rZ| = \frac{1}{\sin(\frac{2\pi}{n})}$. From equation (1), $|\gamma_1^+ v_1^+| < \frac{1}{\sin(\frac{2\pi}{n})}$, and hence v_1^+ is on the open line segment $\gamma_1^+ W$. On the other hand, one can easily observe that the length $|\gamma_1^+ v_1^+|$ increase if and only if the angle $\angle\gamma_3 v_1^+ v_2^+$ increase. Thus, $\angle\gamma_3 v_1^+ v_2^+ < \frac{\pi}{2}$. $\Box$

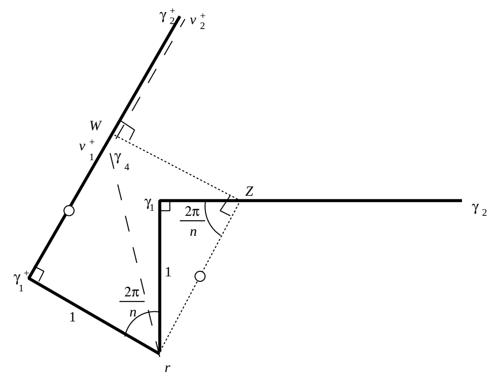

Figure 9. Rectangle $\Box rCD\gamma_1^+$.

For each C_i, the angle $\angle v_1 r\gamma_4$ $(= \angle v_1 r v_1^+)$ is called *the angle of* C_i and may be denoted by $\angle C_i$. A reconfiguration *widen* C_i if it makes the angle $\angle C_i$ increase, and *squeeze* C_i if it makes the angle $\angle C_i$ decrease.

The following lemmas hold.

Lemma 4. *There exists a widened C_i-component if and only if there exists a squeezed C_j-component, where $0 \le i, j \le n-1$ and $i \ne j$.*

Proof. Since $\sum_{i=0}^{n-1} \angle C_i = 2\pi$, the claim immediately holds. $\Box$

Lemma 5. (i) *No reconfigurations can squeeze any C_i-component.*
(ii) *No reconfigurations can widen any C_i-component.*

Proof. (sketch) By Lemma 4, it is sufficient to show only (i).

We may assume, without loss of generality, that the root r is located on the origin of the xy-plane, and the bar $\bar{v_1}$ in C_i is fixed during the reconfiguration. Furthermore, we assume, for a contradiction, that C_i is reconfigured to C_i' such that

$$\angle v_1' r v_1^{+\prime} < \frac{2\pi}{n} = \angle v_1 r v_1^{+}, \tag{2}$$

where the objects (subcomponents, bars and joints) in the C_i'-component are denoted by notations adding the symbol "$\prime$" to the corresponding notations of the objects in the C_i-component.

The bar $\bar{l_2}$ can not swing with the center l_1 both clockwise and counterclockwise since the angles $\angle l_1 l_2 r$ and $\angle l_1 l_2 \gamma_2$ is less than $\frac{\pi}{2}$ from Lemma 3 (i) and (ii). Furthermore, the bar $\bar{\gamma_4}$ can not swing with the center γ_3 both clockwise and counterclockwise since the angles $\angle r\gamma_4\gamma_3$ and $\angle \gamma_3\gamma_4 v_2^{+}$ is less than $\frac{\pi}{2}$ from Lemma 3 (iii) and (iv).

Thus, the only feasible motion is either expanding or reducing the diagonal $\gamma_1\gamma_4$ of the reflex quadrangle $\Box r\gamma_1\gamma_3\gamma_4$. Thus, the following two cases may occur:

Case1: The diagonal $\gamma_1'\gamma_4'$ of the reflex quadrangle $\Box r\gamma_1'\gamma_3'\gamma_4'$ is longer than the diagonal $\gamma_1\gamma_4$ of the initial configuration of the reflex quadrangle $\Box r\gamma_1\gamma_3\gamma_4$; and

Case2: The diagonal $\gamma_1'\gamma_4'$ of the reflex quadrangle $\Box r\gamma_1'\gamma_3'\gamma_4'$ is shorter than the diagonal $\gamma_1\gamma_4$ of the initial configuration of the reflex quadrangle $\Box r\gamma_1\gamma_3\gamma_4$.

Case1: Since $|\gamma_1'\gamma_4'| > |\gamma_1\gamma_4|$, then $\angle\gamma_1' r\gamma_4' > \angle\gamma_1 r\gamma_4$ by the cosine rule for the triangle $\triangle r\gamma_1\gamma_4$. Therefore, by equation (2), $\angle v_1' r\gamma_1' < \angle v_1 r\gamma_1$. This means that the distance between joint γ_1' and bar $\bar{j}_1'(=\bar{j}_1)$ is shorter than the distance between joint γ_1 and bar $\bar{j}_1$. However, the distance between joint γ_1 and bar $\bar{j}_1$ is equal to $|\bar{l_2}|$, and hence $\bar{l_2}$ must cross the path $r\gamma_1\gamma_2$, contradicting a condition of the planar reconfiguration.

Case2: Since $|\gamma_1'\gamma_4'| < |\gamma_1\gamma_4|$, then $\angle\gamma_1' r\gamma_4' < \angle\gamma_1 r\gamma_4$ by the cosine rule for the triangle $\triangle r\gamma_1\gamma_4$, and then $\angle\gamma_4'\gamma_3'\gamma_1' < \angle\gamma_4\gamma_3\gamma_1$ by the cosine rule for the triangle $\triangle\gamma_3\gamma_1\gamma_4$. Therefore, one can easily observe that $\angle\gamma_3'\gamma_1'\gamma_4' > \angle\gamma_3\gamma_1\gamma_4$ and $\angle\gamma_4'\gamma_1' r > \angle\gamma_4\gamma_1 r$. Thus, $\angle r\gamma_1'\gamma_3' < r\gamma_1\gamma_3 = \frac{\pi}{2}$. However, the angle $\angle r\gamma_1\gamma_2$ can not decrease from $\frac{\pi}{2}$, since $\bar{\gamma_2}$ can not swing clockwise, and hence $\bar{\gamma_3}$ must pass through $\bar{\gamma_2}$, contradicting a condition of the planar reconfiguration. $\Box$

Thus, the following theorem holds.

Theorem 1. *There exists a radial tree which can not be straightened.*

6 Conclusion

In this paper, we show that there exists a tree linkage which is radially monotone and can not be straighten. One of the future works is to find a method for straightening tree linkages in other classes.

References

1. T. Biedl, E. Demaine, M. Demaine, S. Lazard, A. Lubiw, J. O'Rourke, S. Robbins, I. Streinu, G. Toussaint, and S. Whitesides, On reconfiguring tree linkages: Trees can lock, In Proceedings of 10th Canadian Conference on Computational Geometry, 1998.
2. T. Biedl, E. Demaine, M. Demaine, S. Lazard, A. Lubiw, J. O'Rourke, S. Robbins, I. Streinu, G. Toussaint, and S. Whitesides, A note on reconfiguring tree linkages: Trees can lock, Discrete Applied Mathematics, vol. 254,pp.19-32,2002.
3. R. Connelly, E. Demaine, and G. Rote, Straightening polygonal arcs and convexifying polygonal cycles, In Proceedings of 41st IEEE Symposium on Foundations of Computer Science, 2000.
4. Y. Kusakari, M. Sato, and T. Nishizeki, Planar Reconfiguration of Monotone Trees, IEICE Trans. Fund., Vol.E85-A, No.5, pp.938-943, 2002.